International Journal of Chemical, Materials and Biomolecular Sciences
ISSN: 2415-6620
Vol:5, No:5, 2011

Theoretical Investigation of Carbazole-Based D-D-π-A Organic Dyes for Efficient Dye-Sensitized Solar Cell

S. Jungsuttiwong[1,*], R. Tarsang[1], S. Pansay[1], T. Yakhantip[2], V. Promarak[1], T. Sudyoadsuk[1], T. Kaewin[1], S. Saengsuwan[1], and S. Namuangrak[3]

***Abstract*—**In this paper, four carbazole-based D-D-π-A organic dyes code as CCT_2A, CCT_3A, CCT_1PA and CCT_2PA were reported. A series of these organic dyes containing identical donor and acceptor group but different π-system. The effect of replacing of thiophene by phenyl thiophene as π-system on the physical properties has been focused. The structural, energetic properties and absorption spectra were theoretically investigated by means of Density Functional Theory (DFT) and Time-Dependent Density Functional Theory (TD-DFT). The results show that nonplanar conformation due to steric hindrance in donor part (cabazole-carbazole unit) of dye molecule can prevent unfavorable dye aggregation. By means of the TD-DFT method, the absorption spectra were calculated by B3LYP and BHandHLYP to study the affect of hybrid functional on the excitation energy (E_g). The results revealed the increasing of thiophene units not only resulted in decreasing of E_g, but also found the shifting of absorption spectra to higher wavelength. TD-DFT/BHandHLYP calculated results are more strongly agreed with the experimental data than B3LYP functions. Furthermore, the adsorptions of CCT_2A and CCT_3A on the TiO_2 anatase (101) surface were carried out by mean of the chemical periodic calculation. The result exhibit the strong adsorption energy. The calculated results provide our new organic dyes can be effectively used as dye for Dye Sensitized Solar Cell (DSC).

***Keywords*—**Dye-Sensitized Solar cell, Carbarzole, TD-DFT, D-D-π-A organic dye

I. Introduction

THE Dye-sensitized Solar Cell (DSC) have attracted a great deal of interest rapidly in the attention of many research groups during the recent years [1]. Since the first developed and reported by M. Grätzel *et al* in the 1991 [2], this DSC technology is one of the most promising alternatives to compete with the traditional silicon solar cell because of organic dye molecules in DSC shown distinguished advantages such as their high optical absorption extinction coefficient, adjustable spectral wavelength response, low cost materials, and their environmental friendly [3, 4]. The mechanism of

[1] Center for Organic Electronics and Alternative Energy (COEA), Department of Chemistry, Faculty of Science, Ubon Ratchathani University, Uon Ratchathani, Thailand 34190 (*Corresponding author Tel.: +66 81 6922125; fax: +66 45 288379; e-mail: jsiriporn_2000@ yahoo.com).
[2] Department of Chemistry, Faculty of Science, Chiang Mai University, Chiang Mai, Thailand 50200.
[3] National Nanotechnology Center, National Science and Technology Development Agency, Klong Luang, Pathumthani, Thailand 10120

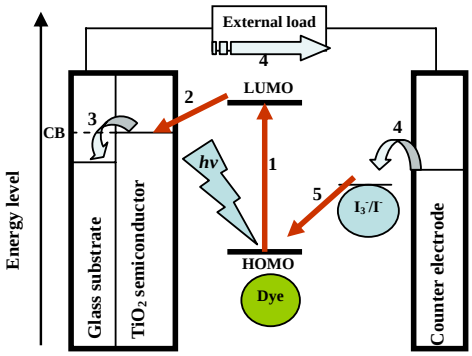

Scheme. 1 Principle operations of DSC: (1) photon excitation; (2) electron injection; (3) electron collection; (4) electron transportation; (5) charge recombination

DSC (shown in scheme 1.) is start when electrons in dye molecules absorb the sun light and go to the excited state (LUMO). The excited electrons are then injected into the conduction band (CB) of TiO_2 via anchoring group in quickly time. These electrons were collected and flow through the external load to the counter electrode, at the same time the oxidized dyes are neutralized to ground state via I_3^-/I^- system. The efficiency of DSC is based on the injection of electrons from dye molecules into the conduction band of TiO_2. Until now, the highest efficiency of DSC reported by M.Grätzel in the early 1990s, which is the ruthenium (Ru) complex coded as N3 dye was recorded about 11% under AM1.5 irradiation and it has used as general reference for standard efficiency of dye [5]. However, the Ru dyes are limited with the problem of manufacturing cost and toxicity issues. Therefore, many research teams have attempted to increase the performance of organic dyes not only in the synthesis laboratory, but also in the field of theoretical investigation based on computational study for understanding mechanism of electron transfer. In recent years, numerous organic dyes, such as coumarin [6], indoline [7], triarylamine [8], perylene [9], and hemicyanine [10] derivatives, have been investigated as dyes in DSC. The efficiency of DSC based on organic dyes is in range of 5-9% that lower than the Ru dyes. One choice for increasing the efficiency of organic dye is the design with Donor-π-conjugated-Acceptor (D-π-A) system [11]. Generally, organic dyes used for efficient DSC are required to broaden spectral absorption with high intensity to get most of sunlight.

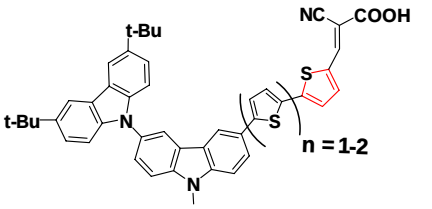

CCT_2A and CCT_3A dyes

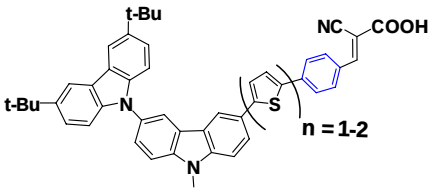

CCT_1PA and CCT_2PA dyes

Scheme 2 Chemical structures of dyes under study

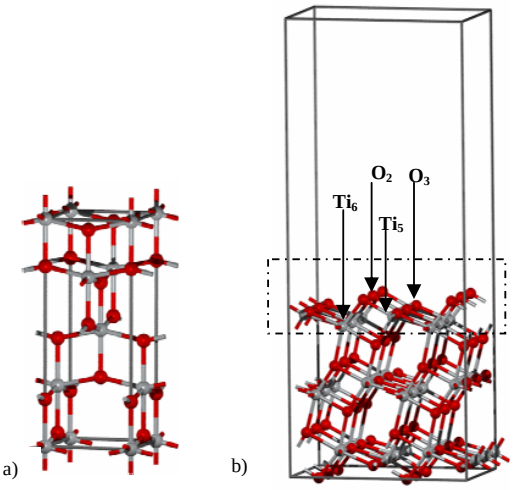

Fig. 1 TiO_2 vacuum slab used for the adsorption studies of the dyes.

And should have suitable energy level by the highest occupied molecular orbital (HOMO) of the dye must lower than iodine/iodide redox potential and the lowest unoccupied molecular orbital (LUMO) must higher than the conduction band of TiO_2. In order to rationalize the experimentally observed properties of known materials as well as predict and design those of unknown efficient-dyes, theoretical studies using accurate quantum mechanical methods are very essential to provide the energetic properties and geometry of the target dye molecules. At present, numbers of papers have been proposed in the theoretical studies of organic dyes for dye-sensitized solar cell [12]. In this study, we reported four carbazole-based D-D-π-A organic dyes CCT_2A, CCT_3A, CCT_1PA and CCT_2PA (show in scheme 2.) which have been synthesized by our group using a combination of bromination, Suzuki coupling and knovenegel condensation reaction. Carbazole dimer acts as electron donor and cyanoacrylic acid as electron acceptor linked by thiophene and phenyl thiophene units as π-spacer. The photophysical properties of dyes, such as structures, and electronic properties, in term of HOMO, LUMO involve the absorption spectra were studied to reveal mechanism of electron transfer and discuss about the efficiency of these dyes. In addition, excitation states and frontier molecular orbitals of dyes were also analyzed. We have also studied the adsorption of CCT_2A and CCT_3A on the TiO_2 anatase (101) surface were carried out by mean of the chemical periodic calculation and analyzed on the adsorption energy.

II. Computational Methods

The calculated results of all organic dyes, CCT_2A, CCT_3A, CCT_1PA and CCT_2PA, have been obtained using Gassian 03 *ab initio* DFT quantum chemical package. The ground-state geometries were fully optimized using Density Functional Theory (DFT) method combined with Becke's three-parameter hybrid functional and Lee-Yang-Parr's gradient-corrected correlation functional (B3LYP) at 6-31G(d,p) level. All calculations were performed without any symmetry constraints only in gas phase. These optimized structures were calculated the first excitation energy (E_g), maximal absorption wavelength and oscillator strengths (f) for the 10 states by using Time-Dependent Density Functional Theory (TD-DFT). To investigate the affect of hybrid functional on the E_g, TD-DFT with B3LYP and BHandHLYP hybrid functional were calculated at 6-31G(d,p) level. Subsequently, the TD-DFT results were entried in to the SWizard program for the simulation of absorption spectra of these dyes. Furthermore, these results are also discussed on electronic transition and its character which related to the absorption wavelength. These calculated results were compared with the experimental data in our group. To model the adsorption modes of the dyes on TiO_2 anatase (101) surface, the periodic density functional theory calculation have been carried out using the Dmol[3] package as implemented in Material Studio (version 4.3). The TiO_2 anatase crystal cell as show in Figure 1.a was cleaved into the (101) surface to form TiO2 periodic slap as show in Figure 1.b. In TiO_2 relaxation, the two lower layers of TiO_2 were fixed to keep their bulk structures and 20 Å vacuum regions between the slab to avoid the surface interaction. For these calculations we used the generalized gradient approximation (GGA) functional with Perdew and Wang (PW91) formulation. The electronic properties of core electron were treated with DFT semi-core pseudopots in term of DNP basis set. The convergence energy tolerance, gradient, and displacement convergences were 1.0 x 10^{-5} Ha, 0.004 Ha/Å, and 0.005 respectively.

III. Results and Discussion

A. Optimal ground-state electronic structures

To gain insight into the effect of differing π-conjugated bridge on geometrical properties of the dye molecules,

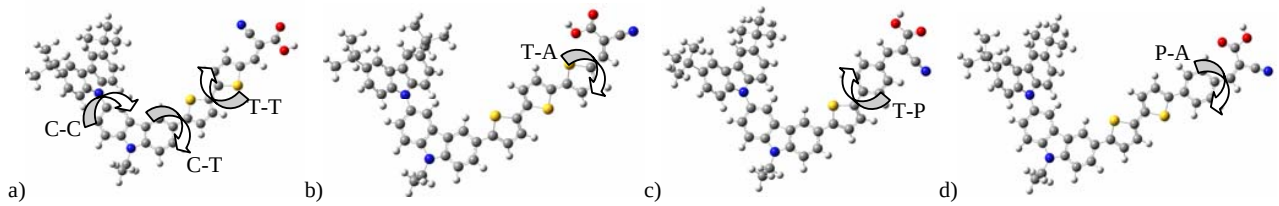

Fig. 2 The optimized conformation of CCT_2A (a), CCT_3A (b), CCT_1PA (c) and CCT_2PA (d) dyes obtained at the B3LYP/ 6-31G(d,p) level.

TABLE I
THE CALCULATED DIHEDRAL ANGLE CORRESPONDING TO THE OPTIMIZED CONFORMATION

Dyes	Dihedral angle (°)							
	C_1-C_2	C_2-T_1	T_1-T_2	T_2-T_3	T_1-P	T_2-P	T-A	P-A
CCT_2A	58.859	26.677	6.817	-	-	-	0.427	-
CCT_3A	58.493	27.962	11.538	6.538	-	-	0.131	-
CCT_1PA	59.057	28.433	-	-	16.204	-	-	0.075
CCT_2PA	56.913	26.862	7.387	-	-	15.245	-	0.105

C = Carbazole, T = Thiophene, P = Phenyl, A = Anchoring group

these four dyes have been optimized using DFT at B3LYP/6-31G(d,p) level of theory, the ground state structures are shown in Fig 2. and the selected dihedral angles are also summarized in Table I. Owing to a major factor for the low conversion efficiency of many organic dyes in the DSC is the formation of dye aggregates on the semiconductor surface [13]. Therefore, we designed carbarzole dimer as donors to perform steric hindrance part of molecules which expect to reduce this dye aggregation phenomenon. For the optimized conformation, we found that dihedral angle between carbazole-carbazole units (in C-C column) of all four dyes were twisted out-of-plane fashion about 58 – 59 degree. These results show that nonplanar conformation due to steric hindrance in dye molecule can prevent unfavorable dye aggregation. Comparing between dyes with two different π-system, one contains only thiophene unit and another one contains phynyl-thiophene moieties, we found that dihedral angle are about 6-7° (T-T column) for the former and 15-16° (T-P column) for the latter. These results indicate that when phenyl ring was introduced to the dyes, the flat conformation on π-system were decreased respect to adjacent ring probably due to steric hindrance with H atom in phenyl ring. This causes the delocalization of π-electrons from donor to acceptor part cannot perform smoothly and may not increase the conjugation length. In addition, dihedral angle between π-spacer and anchoring group (in T-A and P-A column) of CCT_3A, and CCT_2PA are 0.131 and 0.105 degree, respectively, it reveal that replacing thiophene unit by phenyl ring does not significantly affect coplanarity on π-spacer respect to anchoring group of these dyes, consequently the injection of excited electron from thiophene or phenyl thiphene unit into the neighboring cyanoacrylic acid group are conveniently performed which is considered as an intramolecular charge transfer (ICT) process.

B. Effect of intramolecular charge transfer (ICT)

The molecular orbitals contribution is very important in determining the charge-separated states of organic dyes. To create an efficient charge-separated state, HOMO should be localized on the donor subunit, and LUMO should be localized on the acceptor subunit [14]. In order to obtain ICT effect, the density of state (DOS) was performed, the molecular orbitals contribution of four organic dyes were shown in Table2. and the contour plots of HOMO, LUMO and other molecular orbitals of these dyes are displayed in Fig 3. As listed in Table II., we divided the dye molecule into 4 parts, D1, D2, π and A. D1 and D2 represent carbazole units, π represent thiophene or phenyl thiophene unitts and A represent cyanoacrylic acid moeity, we found that electron density of the HOMO were located over the carbazole dimer which are calculated to be 96%(D1-D2), 89%(D1-D2), 97%(D1-D2) and 89%(D1-D2) for CCT_2A, CCT_3A, CCT_1PA and CCT_2PA, respectively. These results show the electron density of HOMO remains delocalized on the donor part. Whereas, the LUMO were located mainly across the π-system and anchoring group which are calculated to be 73%(π), 24%(A) for CCT_2A, 73%(π), 26%(A) for CCT_3A, 67%(π), 31%(A) for CCT_1PA and 73%(π), 26%(A) for CCT_2PA. As shown in Fig 3., molecular orbitals analysis confirmed that the HOMO of all dyes was delocalized over the carbazole dimer and the LUMO was delocalized across the π-system and anchoring group. This distribution of the HOMO and LUMO is separated in the molecule, indicating that the HOMO→LUMO transition can be considered as an intramolecular charge-transfer (ICT) transitions. From TD/BHandHLYP calculated results in Table III., we found that CCT_2A and CCT_1PA show electronic transitions from both of HOMO and HOMO-1 to LUMO. The main character of these transitionscan be assigned as ICT corresponding to the counter plotted of electron density in Fig 3. When thiophene unit of CCT_2A was replaced by phenyl ring in CCT_1PA dye, we found that the electron density in HOMO-1 is delocalized through over the donor and π-system. This results indicating that when electron was excited from HOMO-1→LUMO is composted both of ICT and π-π^* transitions, see in Fig. 3. For CCT_3A and CCT_2PA show similar trend but they also show the composition of HOMO-3

which is ICT character. In addition, the orbitals energies of

Dye	Electronic level	Orbital energies	The percent contribution (%)			
			D1	D2	π	A
CCT_2A	LUMO	-1.85	0	3	73	24
	HOMO	-6.08	76	20	3	0
	HOMO-1	-6.41	13	35	45	7
CCT_3A	LUMO	-1.94	0	1	73	26
	HOMO	-6.05	64	25	11	0
	HOMO-1	-6.25	23	21	53	3
	HOMO-3	-7.01	8	51	35	6
CCT_1PA	LUMO	-1.70	0	2	67	31
	HOMO	-6.07	76	21	3	0
	HOMO-1	-6.44	14	43	40	3
CCT_2PA	LUMO	-1.79	0	1	73	26
	HOMO	-6.01	63	26	11	0
	HOMO-1	-6.22	23	23	52	2
	HOMO-3	-7.00	3	31	56	10

TABLE II
MOLECULAR ORBITALS CONTRIBUTION OF 3 HIGHEST OCCUPIED AND LOWEST UNOCCUPIED MOLECULAR ORBITALS OF CARBAZOLE D-D-π-A ORGANIC DYES
D1, D2 = Carbazole, π = Thiophene or Phenyl thiophene, A = Cyanoacrylic acid

LUMO are -1.85, -1.94, -1.70 and -1.79 eV for CCT_2A, CCT_3A, CCT_1PA and CCT_2PA respectively. These energies level are located above the conduction band (CB) of TiO_2 (2.77 eV) [14] which indicated a good property of dye-sensitizer. Therefore, these CCT_nA organic dyes have sufficient driving force for electron injection into CB of TiO_2.

C. Absorption spectra

To gain insight into the excited states giving rise to the absorption spectra of D-D-π-A organic dyes, TD-DFT calculations were employed with the B3LYP/6-31G(d,p) level in gas phase. It is well known that the failure of TD-DFT/B3LYP in highly delocalized/CT molecules is attributed to the fact that the exchange-correlation potentials generated by the current approximate exchange-correlation function decay too rapidly in the asymptotic region [15]. Therefore, the BHandHLYP functional has been employed to correct asymptotic behavior of the charge transfer (CT) states. The maximal absorption wavelengths from computational results are listed in Table IV. The TD-DFT results were entried into the SWizard program for the simulation of absorption spectra as show in Fig 4. These calculated results were compared with the experimental data in our group. As shown in Table IV. Absorption maximal wavelength of CCT_2A and CCT_3A dye using B3LYP functional are located at 573.40 and 597.46 nm, respectively. It has been shown that when increasing thiophene up to 3 units the adsorption wavelength were red-shifted. The similar trend has been found for the BHandHLYP results, the absorption spectra were located at 405.6 and 423.7 nm for CCT_2A and CCT_3A, respectively, the red-shifted was also performed. However the B3LYP results tended to overestimate the experimental absorption wavelength whereas BHandHLYP can

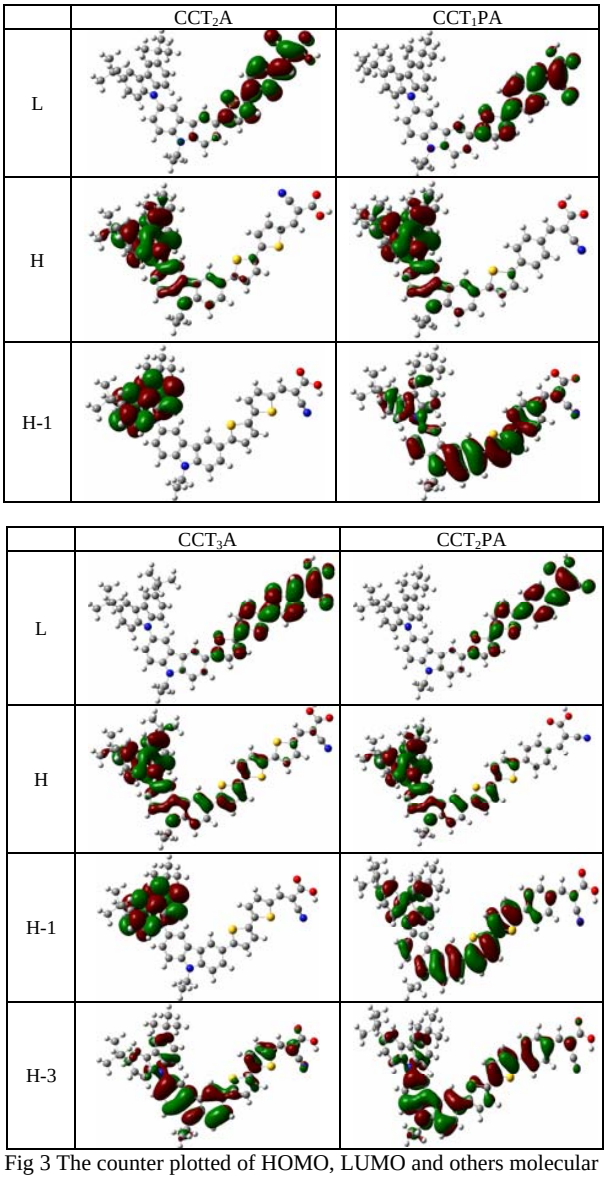

Fig 3 The counter plotted of HOMO, LUMO and others molecular orbitals of D-D-π-A organic dyes

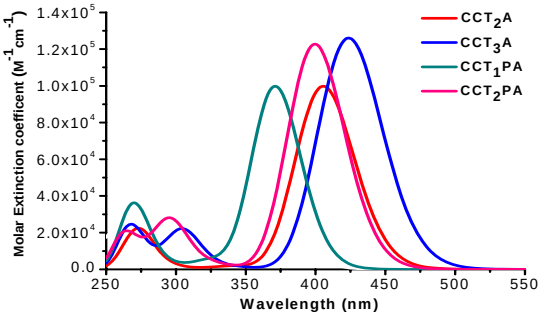

Fig 4 Computational absorption spectra obtained with TD-DFT/ BHandHLYP at 6-31G(d,p)

TABLE III
CALCULATED TD-DFT EXCITATION ENERGY, OSCILLATOR STRENGTH AND ELECTRONIC PROPERTIES OF DYES BY BHANDHLYP/6-31G(D,P)

Dye	State	Excitation energy (eV, nm)	Oscillator strength (*f*)	Assignment	Character
CCT_2A	S1	3.06 (405.6)	1.3781	H-1 → L+0 (+64%)	ICT
				H-0 → L+0 (+14%)	ICT
CCT_3A	S1	2.93 (423.7)	1.7405	H-1 → L+0 (+53%)	ICT
				H-0 → L+0 (+19%)	ICT
				H-3 → L+0 (+8%)	ICT, π-π^*
CCT_1PA	S1	3.34 (371.7)	1.3763	H-1 → L+0 (+59%)	ICT, π-π^*
				H-0 → L+0 (+18%)	ICT
CCT_2PA	S1	3.10 (399.6)	1.6933	H-1 → L+0 (+59%)	ICT, π-π^*
				H-0 → L+0 (+20%)	ICT
				H-3 → L+0 (+7)	ICT, π-π^*

TABLE IV
COMPUTATIONAL AND EXPERIMENTAL ABSORPTION MAXIMA WAVELENGTH

Dye	Calcuation		Experiment
	B3LYP	BHandHLYP	
CCT_2A	573.40	405.6	*N.A.*
CCT_3A	597.46	423.7	443
CCT_1PA	550.32	371.1	420
CCT_2PA	570.64	399.6	425

reasonably improve the calculated results to be more accurate. It has been found that BHandHLYP result is in excellent agreement with experimental data compared with B3LYP results. Furthermore, in Fig 4., the dyes exhibit wide absorption wavelength in range of 250 – 500 nm. For organic dyes with thiophene as π-system CCT_2A and CCT_3A not only show higher absorption wavelenght but also exhibit higher molar extinction coefficient compared to dyes with phenyl-thiophene as π-system (CCT1PA and CCT2PA). In addition, when the number of thiophene unit were increased the increasing of the molar extinction coefficient were found in both of thiophene and phenyl thiophene as π-system.

A. *Adsorption of dyes on TiO_2 anatase (101) surface*

From the above results, it is clear that many properties of CCT_nA dyes with thiophene units as π-system show appropriate more than CCT_nPA dyes which replaced π-system by phenyl ring. For example, CCT_nA dyes show less dihedral angle on conjugated part than the CCT_nPA dyes, low excitation energy, provide good ICT character and also show broaden absorption spectral with high intensity. Therefore, only CCT_nA dyes were used to study the possible adsorption configuration of dyes on the metal oxide due to the strong adsorption configuration play a key role in improving the efficiency of the cell. The adsorption energy, E_{ads} is calculated using the expression

$$E_{ads} = E_{(slab+dye)} - E_{slab} - E_{dye}$$

where E_{slab} represent the energy of the clean slab, E_{dye} represent the achor dye in the gas phase, and $E_{(slab+dye)}$ is the total energy of the complex of the slab with anchor dye. A negative value of $E_{ads} < 0$ indicates stable adsorption. To reduce the computa- tional cost model molecules have been used for the dye-TiO_2 adsorption study by cutting the cabarzole dimer at the first time to calculated all possible adsorption configuration. These configuration include that molecular, dissociative, monodentate via CN-group and bidentate via CN-group and OH-group adsorption mode as show in Fig 5.a, b, c and d, respectively. The values of adsorption energy for possible mode are summarized in Table V, along with importtant structure parameter. From the table, it is observed that the

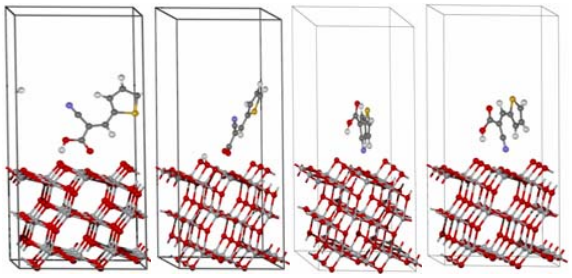

a) b) c) d)

Fig 5 Different possible adsorption modes of anchor dye

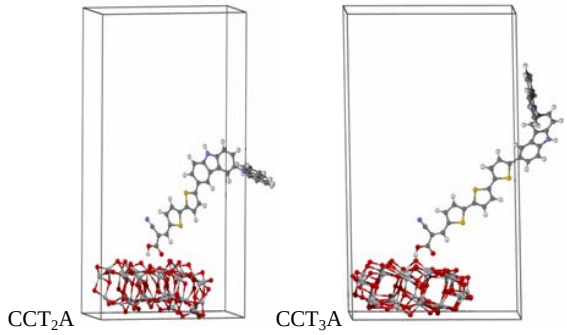

CCT_2A CCT_3A

Fig 6 Molecular adsorption mode of organic dyes on TiO_2 surface

TABLE V
IMPORTANT OPTIMIZED BOND LENGTH (Å) AND ADSORPTION ENERGY FOR THE DIFFERENT ADSORPTION CONFIGURATION OF ORGANIC DYES

Configuration mode	E_{ads} (kcal/mol)	Distance (Å)					
		Ti_{5c}-O	Ti_{5c}-OH	O_{2c}-H	C-OH	C-O	Ti_{5c}-N
a	-25.73	2.182	-	1.508	1.314	1.261	-
b	-22.07	2.029	2.01	0.97	1.275	1.288	-
c	-16.97	-	-	2.947	1.361	1.212	2.251
d	-14.60	-	-	3.892	1.354	1.214	2.308
CCT_2A	-26.11						
CCT_3A	-26.94						

molecular adsorption mode is the most stable by adsorption energy of 25.73 kcal/mol. And then optimized structure for the most stable configuration was extended to perfect molecule as show in Fig 6. These model were reduce TiO_2 in two raw. And we found that both of dyes-TiO_2 complexes show strong adsorption energy by CCT_3A tend to much than CCT_2A dyes.

IV. Conclusion

In summary, the theoretical study of carbazole-based D-D-π-A organic dyes were investigated. To gain a better understanding of the role of its electronic structure, absorption and electron transport properties, we performed DFT and TD-DFT calculation. From the present study, we can infer that CCT_3A dye showed the appropriate donor steric hindrance with coplanarity of π-spacer and anchoring group. It also exhibited the best absorption characteristics in maximum wavelength and highest molar extinction coefficient as well as, performing a good ICT character. Furthermore, it has strong binding energy on TiO_2 surface. This theoretical CCT_3A results show that it could greatly possible to use as potential sensitizer for highly efficient Dye-Sensitized solar cell (DSC). And we found that making use of functional using a larger percentage of exact exchange (BHandHLYP) provided better results for highly delocalized/CT molecules compared to the hybrid B3LYP density functional which tends to overestimate the transition energies. Interestingly, the experimental results obtained from our lab showed that CCT_3A dye performed high efficiency up to 5.76% which is slightly higher than N3 dye 4.11% (DSCs using these four dyes and N3 reference dye as sensitizers with TiO_2 nanoparticle and the electrolyte system of 0.5 M LiI/0.05 M 12/0.4M pyridine in mixture of γ-butyro-lactone (GBL) N-methylpyroridone (NMP) (7:3) were assembled and characterized).

Acknowledgment

The authors would like to express grateful acknowledgments to Department of Chemistry, Faculty of Science, Ubon Ratchathani University. This research was financially supported by the Human Resource Development in Science Project (Science Achievement Scholarship of Thailand, SAST) and Center of Excellence for Innovation in Chemistry (PERCH-CIC).

References

[1] D. Kim, M. Kang, K. Song, S. Kang, J. Ko, "Molecular engineering of organic sensitizers containing indole moiety for dye-sensitized solar cells" *Tetrahedron*, vol. 64, 2008, pp. 10417–10424.
[2] R. Ma, P. Guo, H. Cui, X. Zhang, M.K. Nazeeruddin, M. J. Grätzel, "Substituent Effect on the Meso-Substituted Porphyrins: Theoretical Screening of Sensitizer Candidates for Dye-Sensitized Solar Cells" *Phys. Chem. A*, vol. 113, 2009, pp. 10119-10124.
[3] M. Grätzel, "Photoelectrochemical cells" *Nature*, vol. 414, 2001, pp. 338-344.
[4] M.P. Balanay, D. H. Kim, "DFT/TD-DFT molecular design of porphyrin analogues for use in dye-sensitized solar cells" *Phys. Chem. Chem. Phys.*, vol. 10, 2008, pp. 5121-5127.
[5] M. Grätzel, "Dye-sensitized solar cells" *J. Photochem. Photobiol. C*, vol. 4, 2003, pp. 145-153.
[6] K. Hara, Z.S. Wang, T. Sato, A. Furube, R. Katho, K. Sugihara, Y. Dan-oh, C. Kasada, A. Shinpo, S. Suga, "Oligothiophene-Containing Coumarin Dyes for Efficient Dye-Sensitized Solar Cells" *J. Phys. Chem. B*, vol. 109, 2005, pp. 15476-15482.
[7] T. Horiuchi, H. Miura, K. Sumioka, S. Ushida, "High Efficiency of Dye-Sensitized Solar Cells Based on Metal-Free Indoline Dyes" *J. Am. Chem. Soc.*, vol. 126, 2004, pp. 12218-12219.
[8] G. Li, K.J. Jiang, Y.F. Li, S.L. Li, L.M. Yang, "Efficient Structural Modification of Triphenylamine-Based Organic Dyes for Dye-Sensitized Solar Cells" *J. Phys. Chem. C*, vol. 112, 2008, pp. 11591-11599.
[9] Y. Shibano, T. Umeyama, Y. Matano, H. Imahori, "Electron-Donating Perylene Tetracarboxylic Acids for Dye-Sensitized Solar Cells" *Org. Lett.*, vol. 9, 2007, pp. 1971-1974.
[10] Z.S. Wang, F.Y. Li, C.H. Huang, "Highly efficient sensitization of nanocrystalline TiO2 films with styryl benzothiazolium propylsulfonate" *Chem. Comm.*, 2000, pp. 2063-2064.
[11] L. Zhang, Y. Liu, Z. Wang, M. Liang, Z. Sun, S. Xue, "Synthesis of sensitizers containing donor cascade of triarylamine and dimethylaryl - amine moieties for dye-sensitized solar cells" *Tetrahedron*, vol. 66, 2010, pp. 3318-3325.
[12] R. Ma, P. Guo, L. Yang, L. Guo, Q. Zeng, G. Lui, X. J. Zhang, "A theoretical interpretation and screening of porphyrin sensitizer candidates with anticipated good photo-to-electric conversion performances for dye-sensitized solar cells" *Mol. Str. (Theochem)*, vol. 942, 2010, pp. 131-136.
[13] S.E. Ela, M. Marszalek, S. Tekoglu, M. Can, S. Icli, "Synthesis, characterization and photovoltaic properties of novel molecules based on triarylamine dyes" *Curr. Appl. Phys.*, vol. 10, 2010, pp. 749-756.
[14] Y. Tachinaba, S.A. Haque, I.P. Mercer, J.R. Durrant, D.R. Klug, "Electron Injection and Recombination in Dye Sensitized Nanocrystalline Titanium Dioxide Films: A Comparison of Ruthenium Bipyridyl and Porphyrin Sensitizer Dyes" *J. Phys. Chem. B*, vol. 104, 2000, pp. 1198-1205.

[15] K. Srinivas, K. Yesudas, K. Bhanuprakash, V.J. Roa, L. Giribabu, "A Combined Experimental and Computational Investigation of Anthracene Based Sensitizers for DSSC: Comparison of Cyanoacrylic and Malonic Acid Electron Withdrawing Groups Binding onto the TiO2 Anatase (101) Surface" *J. Phys. Chem. C*, vol. 113, 2009, pp. 20117-20126.